MEMS LITHIUM NIOBATE TRANSFORMER FOR LOW FREQUENCY PASSIVE GAIN WITH HIGH CAPACITIVE LOADS IN ATMOSPHERE

Justin Phelps and Reza Abdolvand
The University of Central Florida, USA

ABSTRACT

This work presents the development, optimization, and characterization of a novel flexural mode piezoelectric transformer utilizing a 128-degree rotated Y-cut lithium niobate on silicon. Targeting low-frequency applications with high capacitance loads, the device was simulated and designed using COMSOL Multiphysics, and subsequently fabricated. The resulting piezoelectric transformer demonstrated an unloaded quality factor of 951 in atmosphere and an effective electromechanical coupling coefficient of 1.78%, resulting in a figure of merit of 17.24. The device exhibited an extracted open circuit gain of 12.7, and a measured gain of 2 was obtained using an oscilloscope with a 0.85nF capacitive load. The device demonstrated an equivalent mechanical inductance of 84.8mH. These findings represent a significant improvement for driving high capacitance loads utilizing piezoelectric transformers.

KEYWORDS

Piezoelectric Transformer, Lithium Niobate, Flexural Mode.

INTRODUCTION

In modern electronics, the ongoing trend towards miniaturization presents significant challenges, particularly in the downsizing of components like transformers. Traditional magnetic transformers, essential for applications such as impedance matching and voltage gain, have encountered scaling challenges due to physical limitations. Advancements have led to the development of thin-film magnetic transformers utilizing standard semiconductor fabrication techniques. However, these transformers are impacted by several performance issues including a notably low quality factor, undesirable magnetic flux-induced noise, and capacitive coupling between coils. These factors collectively degrade the overall system performance in applications employing thin-film magnetic transformers.

A key limitation of thin-film micro transformers is their inherently low inductance values, typically in the nanohenry (nH) range, which results in quality factors only reaching the tens as indicated in the literature [1]. This contrasts sharply with piezoelectric transformers, which can achieve significantly higher quality factors owing to their larger equivalent mechanical inductance, generally in the millihenry (mH) range. Since the energy is transferred acoustically in piezoelectric transformers, they do not suffer from the same magnetic flux leakage problem. Consequently, piezoelectric transformers, using materials such as aluminum nitride, lead zirconate titanate (PZT), and lithium niobate, have been explored as viable alternatives for both impedance matching and voltage gain applications [2, 3, 4].

Despite the potential advantages, MEMS piezoelectric transformers are not without their own drawbacks. Piezoelectric transformers are typically unable to drive capacitive loads larger than 10s of pF while maintaining a voltage gain larger than unity. Most designs in literature are focused on operating in the 10s of Megahertz range.

This paper focuses on a novel approach involving a 128˚ rotated Y-cut, flexural mode lithium niobate-based piezoelectric transformer designed specifically for low frequency applications. We aim to demonstrate that this design can effectively address the limitations encountered with both traditional thin-film magnetic and piezoelectric transformers, offering a solution for passive voltage gain with high capacitance loads.

DESIGN

The design's main objective was to overcome two challenges. The first challenge involved ensuring low frequency operation of the device, while the second focused on its capability to drive high capacitance loads.

The piezoelectric transformer designed utilizes a 128-degree rotated Y-cut lithium niobate to enhance coupling efficiency. The flexural mode, chosen for its reduced equivalent stiffness, allows for lower frequency operation. An elastic silicon layer beneath the piezoelectric material excites the flexural mode, facilitating out-of-plane displacement. Upon electrical excitation, in-plane strain in the lithium niobate induces compensatory bending in the silicon layer. Figure 1 illustrates this bending mechanism and strain interactions.

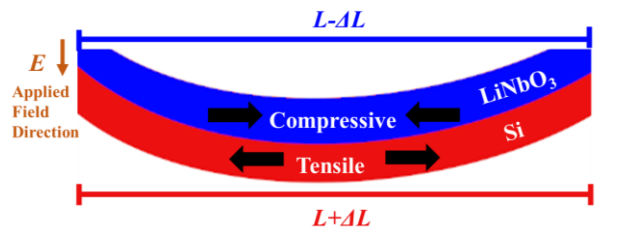

Figure 1: Diagram illustrating out-of-plane bending induced by the silicon elastic layer.

The device was designed and optimized using COMSOL Multiphysics simulator. The initial model consisted of a 2-micron thick 128˚ rotated Y-cut lithium niobate layer atop a 5-micron thick silicon substrate. Within this software environment, an eigenfrequency simulation was conducted to analyze mechanical resonances of the structure. Subsequently, the surface electric potential, induced by mechanical deformations at these eigenfrequencies, was evaluated. The design was further refined by optimizing the in-plane orientation through parametric sweeps, focusing on maximizing the observed electric potential on the surface (Figure 2).

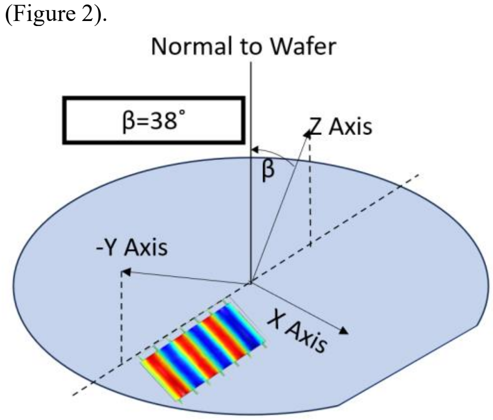

Figure 2: Optimized device in plane rotation on 128˚ rotated Y-cut lithium niobate. Optimum device orientation was found to be perpendicular to the crystal's X axis.

The dimensions and placement of the electrodes were further optimized through parametric sweeps. Tethers to suspend the device were placed at the mechanical nodal points of minimum displacement to minimize acoustic losses shown in Figure 3.

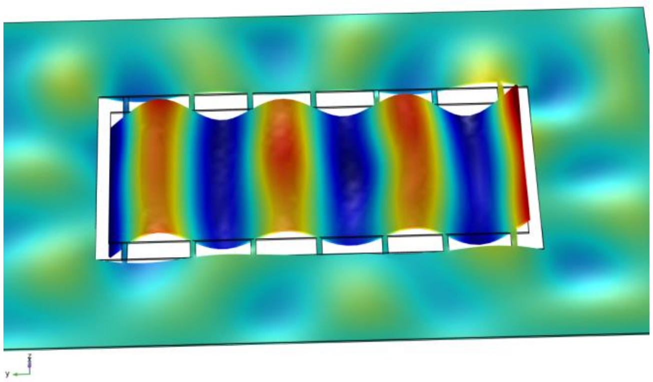

Figure 3: 6th order flexural mode piezoelectric transformer simulation. Color indicates out of plane displacement of the device.

As depicted in Figure 3, due to anchor losses, the support quality factor of the device was simulated to be relatively low (~340). To further enhance this, an isolation frame was designed to surround the device with the objective of confining the energy within the limits of the frame. Through parametric sweeps, the isolation frame geometry was optimized to maximize the quality factor. With the addition of the isolation frame, the simulated quality factor significantly increased to ~1200. Figure 4 depicts the transformer with the optimized isolation frame, where the color scale signifies the surface electric potential polarity: red and blue regions denote positive and negative potentials, respectively. The input/output electrodes are located over the red/blue regions to maximize the energy transferred acoustically from the input to the output electrodes.

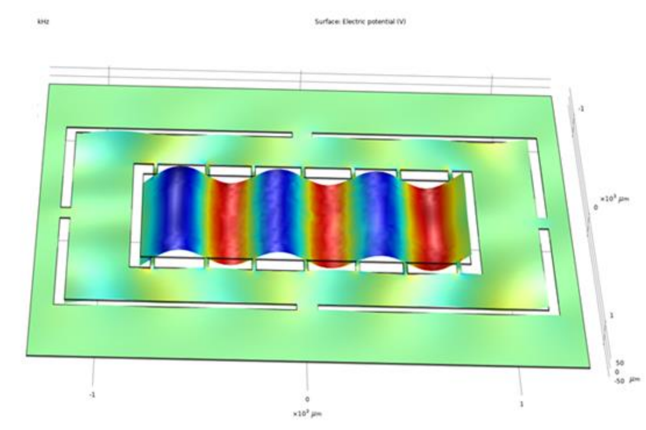

Figure 4: 6th order flexural mode piezoelectric transformer simulation with the isolation frame. Color indicates the surface potential of the device.

The piezoelectric transformer measured 1.6mm in total length and resonated at 325kHZ. Increasing the size further results in lower frequency, however, these dimensions were not increased due to fabrication constraints.

DEVICE FABRICATION

The fabrication process of the piezoelectric transformer, as shown in Figure 5, begins with a bonded 2µm thick lithium niobate layer to a 100nm thick platinum film, which has been sputtered onto a silicon-on-insulator (SOI) wafer with a 5µm thick device layer (Figure 5A). The bonding processes was completed by our industrial partner, "NGK Insulators". The electrodes are patterned using a lift-off technique, where electron beam evaporation is used to deposit 30nm of chromium for adhesion and 100nm of gold (Figure 5B).

Next, the hard mask for etching lithium niobate is prepared. It consists of an unexposed photoresist base layer covered by sputtered nickel. This mask simplifies the nickel removal by lift-off post-etching. The mask is created by spinning a photoresist layer, hard baking at 120°C without exposure, and sputtering 350nm of nickel on top of the photoresist layer. A second photoresist layer is then spun on, baked at 100°C (to prevent reflow of the bottom layer), patterned with direct-write lithography, and developed. The nickel film is chemically etched using a 35°C solution of phosphoric, nitric, and acetic acids diluted in deionized water (Figure 5C).

The underlying photoresist is etched in oxygen plasma to expose the lithium niobate, which is then etched using a reactive ion etcher (RIE) with inductively coupled plasma (ICP), using argon and carbon tetrafluoride (Figure 5D). A lithography step is performed on top of the existing nickel mask to protect the platinum ground electrodes leaving the platinum layer surrounding the device exposed. The device's surrounding platinum layer is etched using argon in an RIE/ICP, and the 5µm silicon layer is etched using SF_6 and C_4F_8 to achieve an anisotropic etch profile (Figure 5E). The nickel hard mask is removed by dissolving the underlying photoresist with acetone thereby lifting off the nickel film.

Finally, to suspend the device, the backside is etched using the Bosch process, stopping at the buried oxide layer of the SOI. The oxide layer is then etched away with buffered oxide etchant, and the device is rinsed in deionized water, followed by methanol to reduce the capillary forces on the released device, and dried in ambient air (Figure 5F). The completed device is shown in Figure 6.

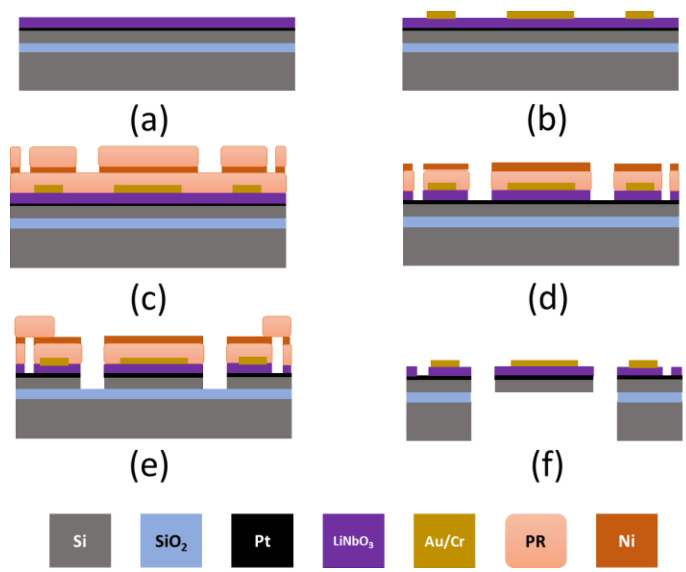

Figure 5: Fabrication process flow for piezoelectric transformer: (a) Initial lithium niobate bonded to Pt on SOI wafer. (b) Electrodes patterned using lift-off. (c) Construction of lithium niobate hard mask. (d) Lithium niobate etched in RIE/ICP. (f) Final released piezoelectric transformer.

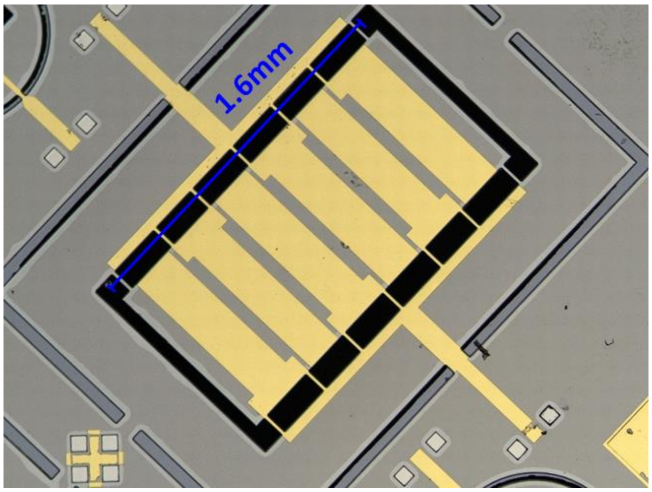

Figure 6: Optical microscope image of the released piezoelectric transformer.

EXPERIMENTAL RESULTS

The completed piezoelectric transformer was next measured using a calibrated probe station and vector network analyzer to measure the scattering parameters of the device which were then exported and modeled in Keysight Pathwave Advanced Design System (ADS). Admittance of the piezoelectric transformer was then plotted, and the Butterworth Van-Dyke (BVD) model was derived for the device (Figure 7) to find the extracted quality factor (*Q*) and k_{eff}^2.

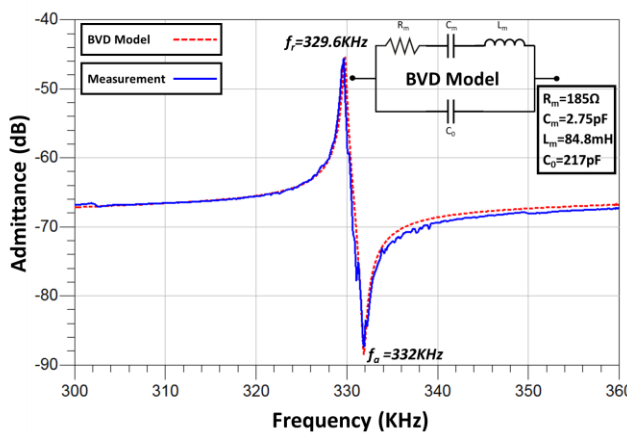

Figure 7: Simulated BVD model and measured admittance of the fabricated piezoelectric transformer.

Based on the BVD model, the unloaded quality factor can be found using the following equation:

$$Q_{Unloaded} = \frac{\omega_r L_m}{R_m} \qquad (1)$$

where ω_r is the resonant angular frequency, L_m is the motional inductance, and R_m is the motional resistance. This calculation results in an unloaded quality factor of 951 in atmospheric conditions. The effective electromechanical coupling (k_{eff}^2) can be calculated based on the resonant (f_r) and anti-resonant (f_a) frequencies obtained from the admittance plot in Figure 7 using:

$$k_{eff}^2 = \left(\frac{\pi^2}{4}\right)\left(\frac{f_a - f_r}{f_a}\right) \qquad (2)$$

Using (2), the effective electromechanical coupling of the device is found to be 1.78%. With the quality factor and effective electromechanical coupling known, the figure of merit (FoM) for the transformer can be calculated as follows:

$$FoM = \frac{Qk_{eff}^2}{\left(1-k_{eff}^2\right)} \qquad (3)$$

Using the unloaded quality factor from the extracted BVD model and the effective coupling measured from the device, the figure of merit for the fabricated piezoelectric transformer is 17.24.

Next, the ability to passively amplify signals was demonstrated for the device. RF probes were used to connect one port of the device to a function generator and the other port of the device to an oscilloscope with a 1 Megaohm input impedance. The combined cabling capacitance was measured to be .85nF (Figure 8). A 50mV$_p$ signal at the resonant frequency of the piezoelectric transformer was applied to the input, and a 100mV$_p$ signal was observed at the output as measured by the oscilloscope (Figure 9).

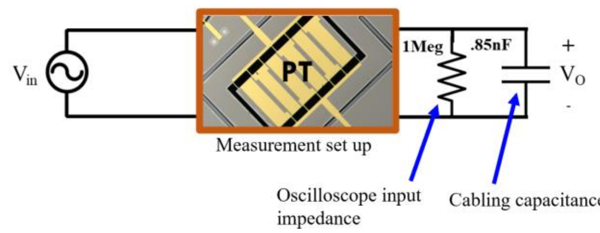

Figure 8: Passive gain measurement configuration. Input voltage signal applied to the piezoelectric transformer (PT) using an RF probe. The output signal was connected from an RF probe to the oscilloscope for measurement.

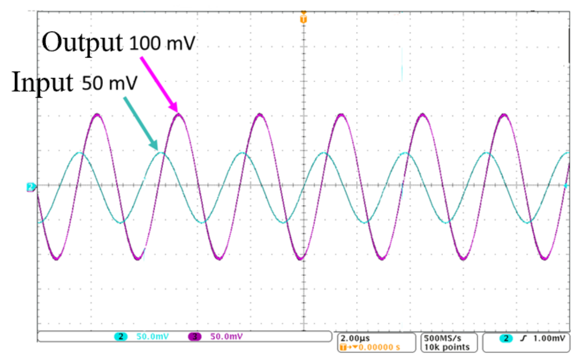

Figure 9: Oscilloscope waveforms showing the input signal to the piezoelectric transformer of 50mV and the output signal of the piezoelectric transformer of 100mV.

Using the extracted BVD model, ADS was used to simulate the effect of various loads on the device. Under open circuit conditions, the maximum gain of the device was found to be 12.7 (22.07 dB). Unity gain (0dB) was found to occur for 2.58nF capacitive loads. The effect of an external matched inductor to cancel out the output capacitance was then simulated. With an inductive load of 1.5mH, the gain was found to be 29.3 (29.34 dB) (Figure 10).

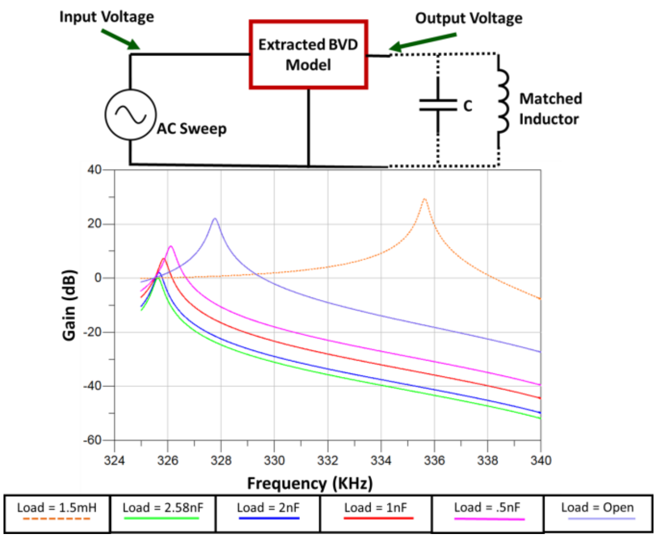

Figure 10: Simulation of piezoelectric transformer's gain under different load conditions. Open circuit, .5nF, 1nF, 2nF, 2.58nF, and a matched 1.5mH inductor are tested.

In Figure 10, it can be seen that as the load changes, the center frequency substantially shifts. This is because the impedance of the load shifts the impedance of the system. For higher capacitive loads, the frequency can be seen to decline. Conversely, adding the matched inductor decreases the effective capacitance thereby increasing the center frequency.

CONCLUSION

This study introduced a novel flexural mode 128-degree rotated Y-cut lithium niobate MEMS piezoelectric transformer, designed for low-frequency operation and high capacitance loads. COMSOL Multiphysics was used to design and optimize the device prior to fabrication. The piezoelectric transformer demonstrated an unloaded quality factor of 951 and an effective electromechanical coupling of 1.78% resulting in a figure of merit of 17.24. The extracted open circuit gain was found to be 12.7 with unity gain occurring for 2.58nF capacitive loads. The device's capability for passive voltage gain was also demonstrated, producing a measured gain of 2 with a load consisting of 0.85nF capacitance in parallel with a 1-Megaohm impedance. The device functions as a 1:1 transformer with the gain resulting from the quality factor of the device. Future work may focus on altering the ratios of the input and output electrode areas for impedance matching applications.

REFERENCES

[1] Bajwa, Rayan, and Murat Kaya Yapici. "Integrated on-chip transformers: recent progress in the design, layout, modeling and fabrication." *Sensors* 19.16 (2019): 3535.

[2] Fatemi, Hediyeh, and Reza Abdolvand. "High-frequency thin-film piezoelectric transformers." *2012 IEEE International Frequency Control Symposium Proceedings*. IEEE, 2012.

[3] Bedair, Sarah S., et al. "Boosting MEMS piezoelectric transformer figures of merit via architecture optimization." *IEEE Electron Device Letters* 39.3 (2018): 428-431.

[4] Manzaneque, Tomás, et al. "A high FoM lithium niobate resonant transformer for passive voltage amplification." *2017 19th International Conference on Solid-State Sensors, Actuators and Microsystems (TRANSDUCERS)*. IEEE, 2017.

CONTACT

*Justin Phelps: justin.phelps@ucf.edu